

*Regular article*

# The hierarchy of localization basins: a tool for the understanding of chemical bonding exemplified by the analysis of the $\text{VO}_x$ and $\text{VO}_x^+$ ( $x = 1-4$ ) systems

M. Calatayud<sup>1</sup>, J. Andrés<sup>1</sup>, A. Beltrán<sup>1</sup>, B. Silvi<sup>2</sup>

<sup>1</sup> Departament de Ciències Experimentals, Universitat Jaume I. Box 224, 12080 Castelló, Spain

<sup>2</sup> Laboratoire de Chimie Théorique, Université Pierre et Marie Curie, 4 Place Jussieu, Paris 75252 cédex 05, France

Received: 20 July 2000 / Accepted: 20 October 2000 / Published online: 23 January 2001

© Springer-Verlag 2001

**Abstract.** The hierarchy of the electron localization basins is a powerful tool of analysis of the bonding in molecules and solids within the “elfological” framework. It is a generalization of the molecular isodensity contour analysis originally proposed by Mezey. In this approach the basins are ordered with respect to the electron localization function values at the critical points which determine the reduction of the reducible localization domains. The procedure enabling the corresponding tree diagrams to be built is described and it is shown how the method can be used as a generator of mathematical definitions of chemical concepts. The possibility offered by this simple tool is illustrated by a study of the  $\text{VO}_x$  and  $\text{VO}_x^+$  ( $x = 1-4$ ) oxides in their ground state and in some excited states.

**Key words:** Vanadium oxides – Clusters – Bonding – Electron localization function – Topological analysis

## 1 Introduction

The electron localization function (ELF) of Becke and Edgecombe [1] is an acknowledged tool for the description and the understanding of the bonding in molecules and solids [2]. This function provides a local measure of the efficiency of the Pauli repulsion with respect to the homogeneous electron gas gauge and therefore enables the recognition of which regions of a molecule are dominated by the antiparallel spin pair behavior. The pictures of the chemical systems depicted by the ELF are

always consistent with the expectation, which can be inferred from the Lewis theory [3, 4], and from the valence-shell electron-pair repulsion model [5–7]. A step forward has been accomplished by achieving the partition of the molecular space in terms of the basins of ELF attractors [8]. This approach is inspired by the theory of “atoms in molecules” of Bader [9], in which the one-electron density distribution is used as the potential function of the gradient dynamical field, which yields the direct space partitioning of the molecule into atoms. The introduction of the topological approach in the ELF analysis not only gives access to qualitative information but also to quantitative information, such as the basin populations and their covariance [10, 11]. Moreover some people involved in the ELF business have been convinced that the topological approach is a key for the improvement of the definitions of chemical concepts. Most of the chemical concepts related to the bonding – such as bond, lone pair, covalency, ionicity – rely on an intuitive representation of the matter rather than on observable quantities. In this respect they belong much more to some kind of natural history rather than to exact science thinking. This led to the consideration of the gradient dynamical field of the ELF as a possible mathematical model of the Lewis theory. In this context, the gradient dynamical system itself as a mathematical structure becomes the principal element of the theory pushing the ELF into the middle ground. The exploration of the mathematical properties of the gradient dynamical systems enables one to find that the isomorphism with our standard representation of the chemistry is not only limited to a static view of the bonding but can be extended to a dynamical one such as in the description of chemical reactions by catastrophe theory [12]. It is then possible to propose nonambiguous definitions of covalent and dative bonds [12] and moreover to establish predictive rules for protonation [13] on the basis of the structural stability of the gradient field.

The sole gradient dynamical system mathematical properties do not provide the whole set of definitions

Correspondence to: A. Beltrán

Contribution to the Proceedings of the 2000 Symposium on Chemical Bonding: State of the Art in Conceptual Quantum Chemistry

necessary to describe the bonding in molecules and, therefore, some other mathematically based approaches are required for this propose. The topological concept of the domain was introduced in chemistry by Mezey [14] in order to recognize functional groups within organic molecule. Generalized to ELF isovalues this concept has proved to be an efficient “generator” of clear definitions. This article focuses on this particular aspect of “elfology” (according to Weyrich’s neologism introduced in his conclusions of the La Colle sur Loup Conference). Our purpose is to give a synthesis of the use of domains in the ELF analysis framework, to provide the technical recipes and to discuss the nature of the chemical information gained by this technique. As an illustration of the method we present an analysis carried out on the  $\text{VO}_x$  and  $\text{VO}_x^+$  systems in their ground state and in some excited states.

## 2 The ELF topological analysis and the concept of domain

As already stated in the Introduction the topological analysis of ELF is intended to provide a direct space mathematical model to Lewis theory. This implies the following assumptions:

1. It is chemically meaningful to perform a partition of the direct space in order to recover a one-to-one correspondence with the localized electron pair of Lewis.
2. The basins of the gradient systems of an ad hoc potential function are best-suited mathematical objects for this purpose.
3. There exists such a potential function, which we call the localization function,
4. The ELF is a good approximation of the ideal localization function.

These assumptions have nothing to do with quantum mechanics and therefore one can consider the mathematical model provided by the ELF gradient field as independent of quantum mechanics; however, to be valid the approach never contradicts the postulates of quantum mechanics. For these reasons, the localization function, which carries all the physical information, should fulfill several requirements so as to be expressible in terms of the exact wave function and to be totally symmetric with respect to the operation of the molecular point group. With this respect the ELF is satisfactory. Moreover in its basic formulation the analysis is restricted to clamped nuclear configurations: in other words the nuclear positions are parameters of the localization function.

### 2.1 The ELF

The original expression of the ELF is

$$\eta(\mathbf{r}) = \frac{1}{1 + \left(\frac{D_\sigma}{D_\sigma^0}\right)^2}, \quad (1)$$

in which  $D_\sigma$  and  $D_\sigma^0$  represent the curvature of the electron pair density for electrons of identical  $\sigma$  spins

(the Fermi hole) for the actual system and a homogeneous electron gas with the same density, respectively. The analytical form of the ELF confines its values between 0 and 1.

$D_\sigma$  is the excess local kinetic energy due to Pauli repulsion.  $D_\sigma$  is a positive quantity which is small in regions of space where the electrons do not experience the Pauli repulsion, that is where the electrons are alone or form pairs of antiparallel spins or where the parallel spin electrons are far from one another; it is large where they are close to one another. The original derivation of the ELF considers the Laplacian of the Hartree–Fock (HF) conditional probability of finding a  $\sigma$ -spin electron at position  $\mathbf{r}_2$  when a first  $\sigma$ -spin electron is located at  $\mathbf{r}_1$ .

$$D_\sigma = [\nabla_2^2 P_{\text{cond}}^{\sigma\sigma}(1, 2)]_{1=2} = \sum_{i=1}^N |\nabla \varphi_i|^2 - \frac{1}{4} \frac{|\nabla \rho^\sigma(1)|^2}{\rho^\sigma(1)} \quad (2)$$

From a rigorous point of view this expression of the ELF is only valid for closed-shell systems described by a single determinant. However, when Eq. (2) is used for open-shell systems acceptable results have been obtained, yielding similar atomic shell populations compared to those obtained with a spin-polarized formula [15] and, therefore, most applications on radicals can be carried out with the standard Eq. (2). In practice, rather than  $D_\sigma$  we use  $D_\sigma + \varepsilon$  where  $\varepsilon$  is an arbitrary small quantity (typically of the order of  $10^{-5}$ ) in order to force  $\eta(\mathbf{r})$  to tend to zero when the electron density vanishes.

### 2.2 The basins of the ELF gradient field

The topological analysis of the ELF gradient field relies on the normal analogy of this field with a velocity field i.e.  $\nabla \eta(\mathbf{r}) = d\mathbf{r}/dt$ . For each point of the molecular space the time integration determines a unique trajectory which starts and ends in the neighborhood of points for which  $\nabla \eta(\mathbf{r}) = 0$ , the  $\alpha$  and  $\omega$  limits, respectively. Such points, called critical points, are characterized by their indexes  $I(m)$  (the number of positive eigenvalues of the second derivative matrix). The stable manifold or inset of a critical point is the set of all points for which this critical point is an  $\omega$  limit; the unstable manifold or outset is the set of points for which this critical point is an  $\alpha$  limit. The stable manifold of a critical point of index 0 (a local maximum or attractor) is the basin of the attractor; that of a critical point of index larger than 0 is a separatrix: it is the boundary between basins. There are basically two types of basins. On the one hand, there are core basins organized around nuclei (with  $Z > 2$ ) and, on the other hand, there are valence basins in the remaining space. The structure provided by the core basins closely matches the inner atomic shell structure. A valence basin is characterized by its synaptic order, which is the number of cores to which it is connected [10], provided these core basins are surrounded by the same localization domain (vide infra).

From a quantitative point of view the method enables the calculation of the basin populations

$$\bar{N}_i = \int_{\Omega_i} \rho(\mathbf{r}) d\mathbf{r} \quad (3)$$

and the variance of the basin populations [10, 11]

$$\sigma^2(\Omega_i) = \int_{\Omega_i} d\mathbf{r}_1 \int_{\Omega_i} \pi(\mathbf{r}_1, \mathbf{r}_2) d\mathbf{r}_2 + \bar{N}_i - \bar{N}_i^2, \quad (4)$$

in which  $\pi(\mathbf{r}_1, \mathbf{r}_2)$  denotes the spinless pair density. The basin population variance is a measure of the quantum mechanical uncertainty and, therefore, an indicator of the electron delocalization. It has been shown [11] that  $\sigma^2(\Omega_i)$  can be expressed in terms of the contributions arising from the other basins (covariance), i.e.

$$\sigma^2(\Omega_i) = \sum_{j \neq i} \bar{N}_i \bar{N}_j - \bar{N}_{\{i,j\}} = \sum_{j \neq i} C_{\{i,j\}}, \quad (5)$$

in which  $\bar{N}_{\{i,j\}}$  is the actual number of pairs between the  $\Omega_i$  and  $\Omega_j$  basins. High values of the covariance  $C_{\{i,j\}}$  indicate large delocalization between the two basins.

### 2.3 The localization domains

#### 2.3.1 Definitions

In topology a domain is defined as follows: let  $M'$  be a subset of the manifold,  $M$ . If for any couple of points  $a$  and  $b$  there exists a path joining  $a$  and  $b$  totally contained in  $M'$  then  $M'$  is a domain. Any subset of the molecular space bounded by an external closed isosurface  $\eta(\mathbf{r})=f$  is a domain. An  $f$ -localization domain is such a subset with the restriction that each point satisfies  $\eta(\mathbf{r}) > f$ .

If an  $f$ -localization domain surrounds at least one attractor it is called irreducible. If it contains more than one attractor it is reducible. An irreducible domain is a subset of a basin, whereas a reducible one is the union of subsets of different basins. Except for atoms and linear molecules, the irreducible domains are always full balls, whereas the reducible ones can be either full balls or donuts. Upon the increase of the value of  $\eta(\mathbf{r})$  defining the bounding isosurface, a reducible domain splits into several domains each containing fewer attractors than the parent domain. The reduction of localization occurs at turning points, which are critical points of index 1 located on the separatrix of two basins involved in the parent domain. Ordering these turning points (localization nodes) by increasing  $\eta(\mathbf{r})$  enables tree diagrams to be built reflecting the hierarchy of the basins.

#### 2.3.2 What can we learn from the localization domains?

From the chemical point of view the localization domain are very useful to discuss the bonding in molecules and in complexes. Three types of domains can be distinguished according to the nature of the attractors within them. A core domain contains the core attractor(s) of given atoms, a valence domain only valence attractors and a composite domain both valence and core ones. For any system there exist low values of  $\eta(\mathbf{r})=f$  defining a unique composite parent domain. The successive reductions of localization split this parent domain. Every child who is a composite domain corresponds to one or more chemical species. In a complex such as in a weak hydrogen bonded system the first reduction yields

two composite domains corresponding to the interacting moieties; therefore, such a complex cannot be considered as being chemically bonded [16].

In a molecule the initial parent domain first splits into core domains and a single valence domain which contains all valence attractors. The shape of this latter domain is that of an empty ball with as many holes as atomic cores in the molecule. Each hole contains a core domain. A core contributes to the synaptic orders of the adjacent valence basin if the value of the localization function determines a core domain occupying such a hole. Ionic pairs follow two parallel behaviors according to the nature of the cation. In the case of alkaline and alkaline-earth cations a reduction of localization occurs for about  $\eta(\mathbf{r}) \approx 0.03$ , which separates the core domain of the cation from the remaining (anionic) composite domain. This latter is reduced in irreducible domains at higher ELF values. For transition-metal compounds the ELF value on the core–valence separatrix is much higher, about 0.2, and, therefore, core–valence separation in the ionic moiety occurs at a lower value than the cation–anion one. Several reasons can explain this behavior. On the one hand, the orbital contribution to the transition-metal core shows a noticeable contribution of the partially empty  $d$  orbitals, which also contribute to the atomic valence shell to a lesser extent. As a consequence of the ambivalent character of the  $d$  orbitals, the electron delocalization between the external core and the valence shells is larger than for main-group elements. On the other hand, the external core shell basin attractor corresponds to a lower ELF value than in main-group elements of the same row because the unpaired electrons are mostly localized within it.

The successive reductions of the molecular valence domain are closely related to functional groups (this was already pointed out for the electron density domains by Mezey [14]) and also to the in situ atomic electronegativities [17, 18]. This is exemplified by methanol. The localization reduction diagram clearly shows that the first reduction of the molecular valence domain gives rise to two reducible domains, which can be assigned to the methyl group and the alcohol function, respectively. At higher ELF values, as shown in Fig. 1, the methyl and alcohol domains are totally reduced. It is worth nothing that the separation of the  $V(\text{C}, \text{O})$  domain from the oxygen atom valence domain takes place at a higher ELF value than that involving the methyl  $V(\text{C}, \text{H})$  domains, which is consistent with the relative electronegativities of the carbon and oxygen centers.

## 3 Computational procedure

The calculations were performed with the GAUSSIAN94 program package [19]. The molecular properties were studied in the framework of density functional theory using Becke's three-parameter hybrid functional [20, 21]. The wave functions of the systems were computed at the restricted HF or unrestricted HF levels and the 6-31G\* basis set developed by Rassolov et al. [22] was used. The low-lying spin states, i.e. singlet, doublet, triplet and quadruplet, of a given cluster were considered in the calculations and the corresponding potential-energy surfaces for the different electronic states were explored in detail.

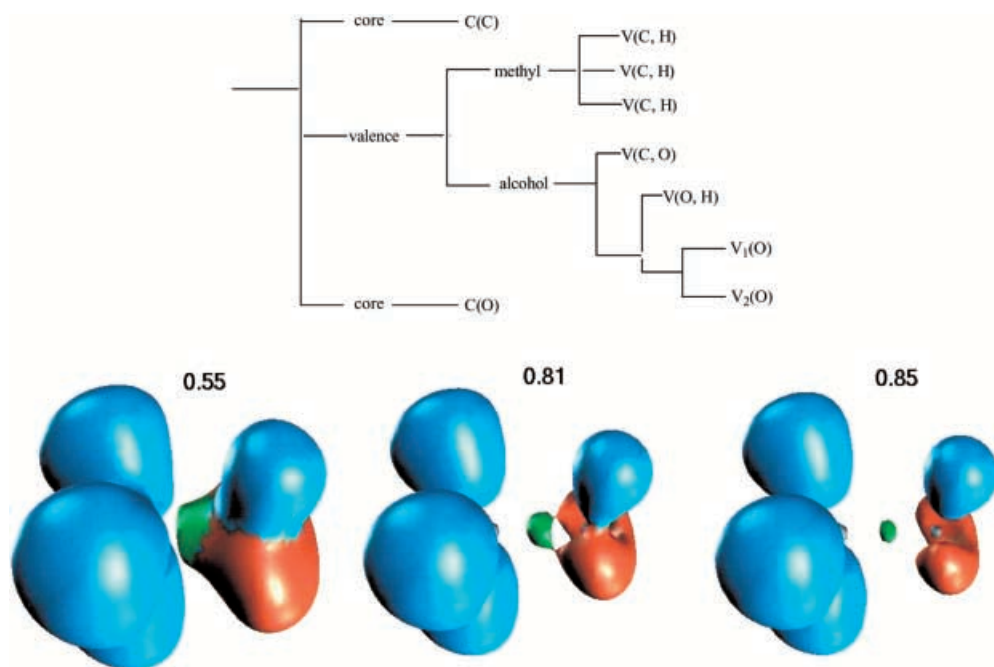


**Fig. 1.** Localization domains of methanol for  $\eta(\mathbf{r})=0.55, 0.81$  and  $0.85$

The nature of each stationary point, minima and transition structures (TSs), was established by calculating analytically and diagonalizing the matrix of the energy second derivatives to determine the number of negative eigenvalues, zero for local minima and one for a TS.

#### 4 Results and discussion

The structures of the minima and some TSs on the corresponding potential-energy surfaces for the  $\text{VO}_x^+$  and  $\text{VO}_x$  ( $x=1-4$ ) clusters and the atoms numbering are displayed in Figs. 2 and 3, respectively. A schematic representation of relative energy for each electronic state of the different clusters is presented in Fig. 4.

Knowledge of the chemical nature of the vanadium oxides is crucial to the understanding of their reactivity. The ELF analysis of the vanadium oxide clusters relies upon the analysis of the bifurcations of the localization domains. The localization domains are then ordered regarding the ELF critical values yielding bifurcations. The hierarchy of the bifurcation can be visualized by a tree diagram. Tree diagrams for the most stable structures of each cluster and for the oxygen molecule are depicted in Fig. 5, while in Fig. 6 some excited electronic states are considered. The partition/bifurcation of the core and valence domains is called the core/valence bifurcation. It can occur in two different ways: either the core irreducible domains split before the valence ones or the core/valence separation takes place after the valence division in two or more domains. The first process is characteristic for molecules or ions, while the second one is characteristic for weak interactions among fragments.

##### 4.1 $\text{O}_2$

The bifurcation tree diagram for the oxygen molecule shows the core–valence splitting at  $\eta(\mathbf{r})=0.150$ , while

another valence domain division involving one disynaptic and two monosynaptic basins takes place at an ELF value of 0.692. It is important to notice the presence of a disynaptic basin  $V(\text{O}_1, \text{O}_2)$  representing a covalent bond between the two oxygens. Monosynaptic basins represent oxygen nonbonding electrons (lone pairs). The ELF isosurface is presented in Fig. 7.

##### 4.2 $\text{VO}^+$ and $\text{VO}$

The  $\text{VO}^+$  ( $^3\Sigma$ ) tree diagram shows a core/valence bifurcation at  $\eta(\mathbf{r})=0.25$ , with a valence splitting into a vanadium core and a monosynaptic oxygen basin. An analysis of the results shows that the valence basin is monosynaptic and is associated with the oxygen lone pairs; therefore, the interactions between V and O atoms can be described as purely ionic. A similar tree diagram is obtained for the excited  $\text{VO}^+$  ( $^1\Delta$ ).

$\text{VO}$  ( $^2\Sigma$ ) presents a core/valence bifurcation for an ELF value of 0.15, and the valence basin splits at an ELF value of 0.2 into a vanadium valence basin and another valence domain which at  $\eta(\mathbf{r})=0.38$  divides into the vanadium core and the monosynaptic oxygen valence basin. The lack of disynaptic  $V(\text{V}, \text{O})$  basins allows us to consider an ionic interaction of vanadium and oxygen atoms. Similar behavior is found for the excited quadruplet,  $\text{VO}$  ( $^4\Sigma$ ).

##### 4.3 $\text{VO}_2^+$ and $\text{VO}_2$

The  $\text{VO}_2^+$  ( $^1A_1$ ) and  $\text{VO}_2$  ( $^2A_1$ ) tree diagrams are analogous to the previous  $\text{VO}^+$  ( $^3\Sigma$ ) and  $\text{VO}$  ( $^2A_1$ ) clusters, respectively, with similar ELF values for the corresponding splitting. In these cases ionic interactions are responsible of the bonding between vanadium and oxygen atoms.

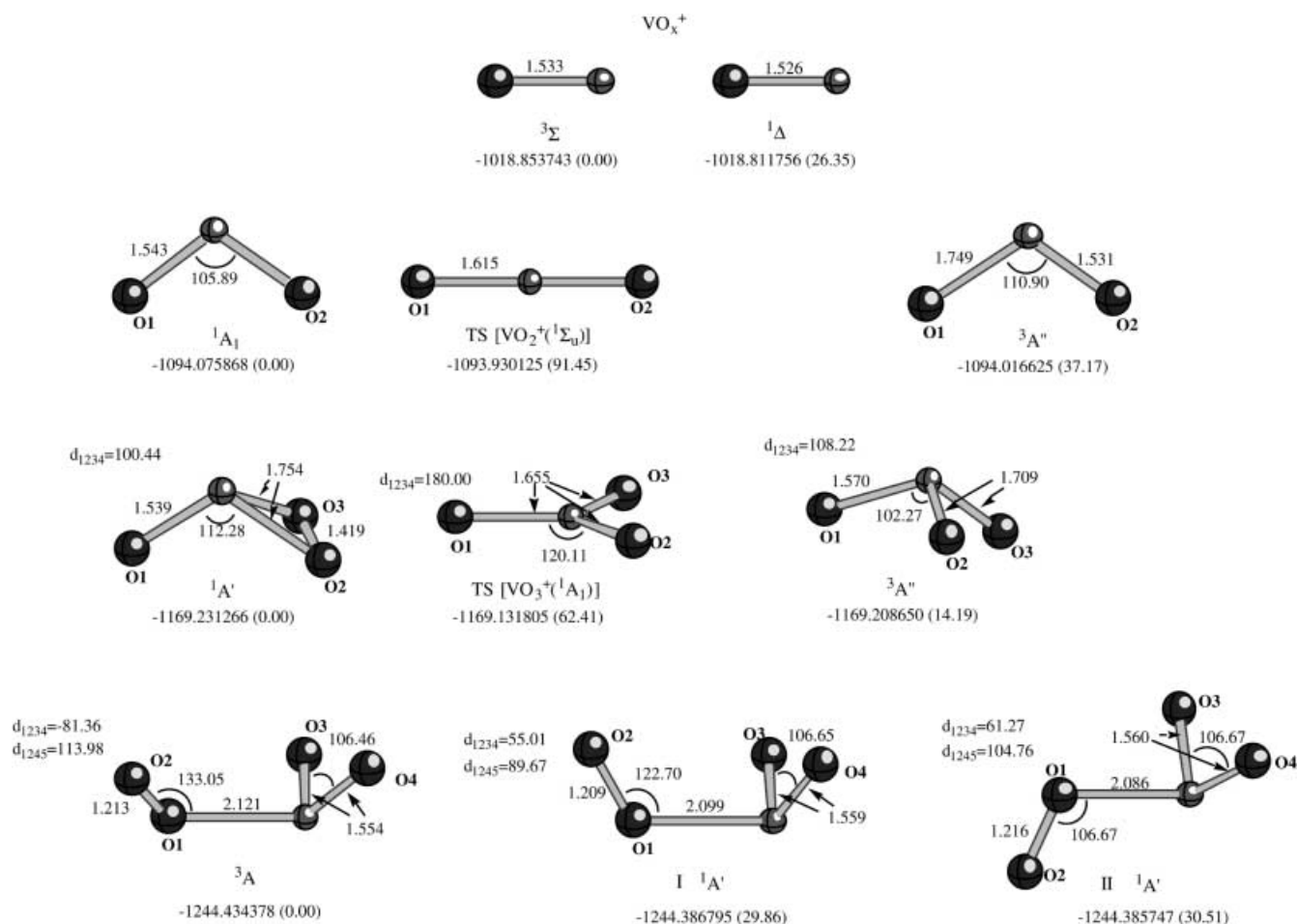


**Fig. 2.** Geometrical parameters (distances in Angstroms and bond angles in degrees), for  $\text{VO}_x^+$  systems in different electronic states

The tree diagram for the excited state  $\text{VO}_2^+$  ( $^3A''$ ) renders a valence bifurcation at  $\eta(\mathbf{r})=0.25$  corresponding with the split of one oxygen, while at  $\eta(\mathbf{r})=0.40$  a core/valence bifurcation appears that divides into a vanadium core and a monosynaptic oxygen valence basin. There is a TS in the energy surface, in the singlet and ground electronic state, TS [ $\text{VO}_2^+(^1\Sigma_u)$ ] connecting two identical minima with an energy barrier of 91.45 kcal $\cdot\text{mol}^{-1}$ . The corresponding tree diagram is similar to that of  $\text{VO}_2^+$  ( $^3A''$ ) with different values of  $\eta$  for both bifurcation points.

A detailed exploration of the potential-energy surface shows the presence of a TS, TS [ $\text{VO}_2^+(^2\Sigma_u)$ ], associated with a bending mode connecting the two identical minima in the doublet electronic state; the corresponding value of the interconversion barrier height is 24.02 kcal $\cdot\text{mol}^{-1}$ . An analysis of the tree diagram shows the absence of a monosynaptic vanadium valence basin.

A comparison of the tree diagram of the fundamental,  $\text{VO}_2$  ( $^2A_1$ ), and the excited state,  $\text{VO}_2$  ( $^4A''$ ), shows the presence of the monosynaptic vanadium valence basin at  $\eta(\mathbf{r})=0.3$  and  $\eta(\mathbf{r})=0.13$ , respectively. However, two different V–O distance values are present in  $\text{VO}_2$  ( $^4A''$ ); therefore, in its tree diagram a core/valence bifurcation appears that divides into a vanadium core

and the monosynaptic oxygen valence basin at two different values of  $\eta$ , 0.20 and 0.36.

#### 4.4 $\text{VO}_3^+$ and $\text{VO}_3$

$\text{VO}_3^+$  ( $^1A'$ ) presents an interesting bifurcation diagram. We observe the core/valence division at low ELF values, and at  $\eta(\mathbf{r})=0.31$  two different domains appear, corresponding to a VO and an  $\text{O}_2$  unit. The former splits at  $\eta(\mathbf{r})=0.40$  into a C(V) and a V(O) basins, analogous to the  $\text{VO}^+$  ( $^3\Sigma$ ) analysis; the latter splits at  $\eta(\mathbf{r})=0.68$  into valence monosynaptic basins for oxygens numbers 2 and 3, and a small disynaptic V(O2,O3) domain appears, splitting at a close value into two small monosynaptic basins. This bifurcation pattern is very similar to the  $\text{O}_2$  molecule one; therefore, we consider  $\text{VO}_3^+$  ( $^1A'$ ) as an ionic interaction between a  $\text{VO}^+$  ( $^3\Sigma$ ) and an  $\text{O}_2$  molecule. This description can be observed pictorially in the isosurface representation of Fig. 8. A similar diagram to that of the ground state,  $\text{VO}_3^+$  ( $^1A'$ ), appears for the excited  $\text{VO}_3^+$  ( $^3A''$ ) but in this case the corresponding disynaptic basin of the oxygen molecule is not present, while for the TS no split of core/valence basin is obtained.

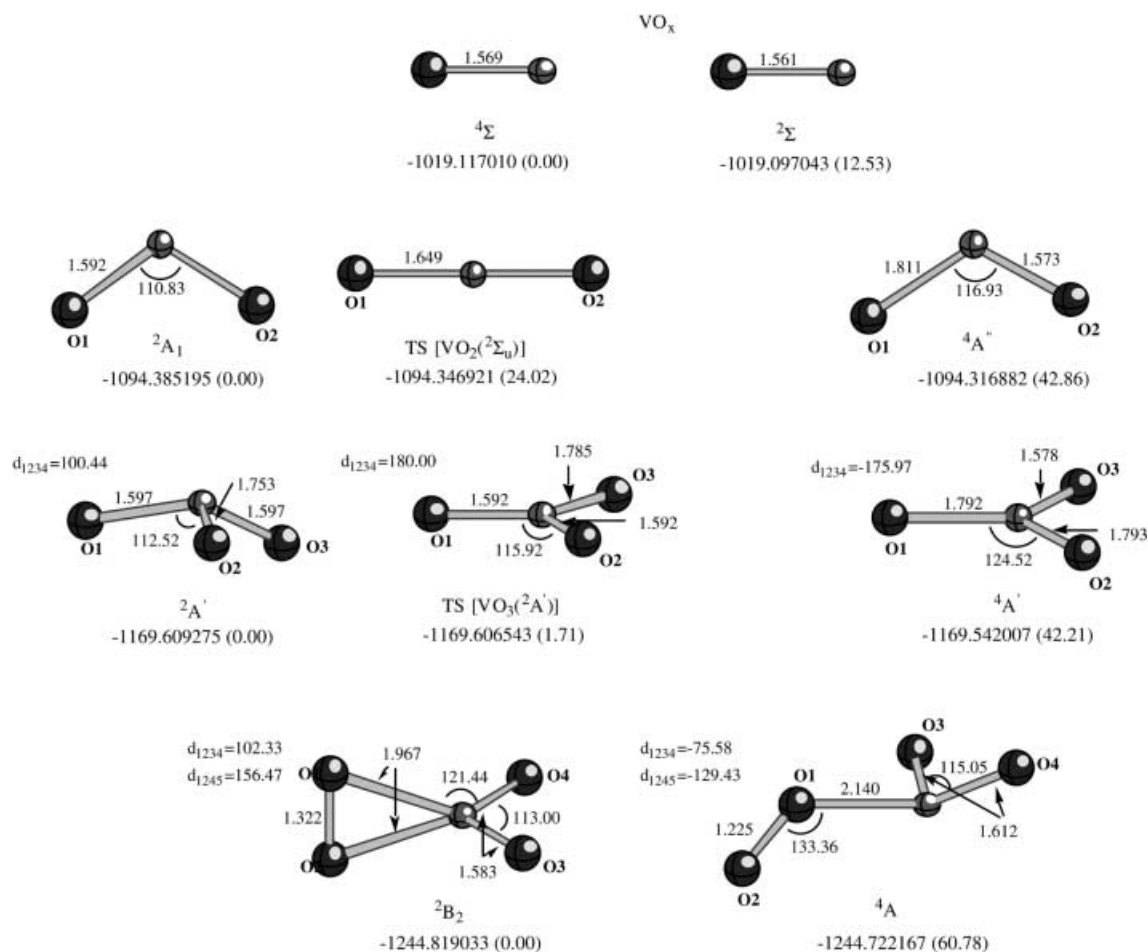


Fig. 3. Geometrical parameters (distances in angstroms and bond angles in degrees), for  $\text{VO}_x$  systems in different electronic states

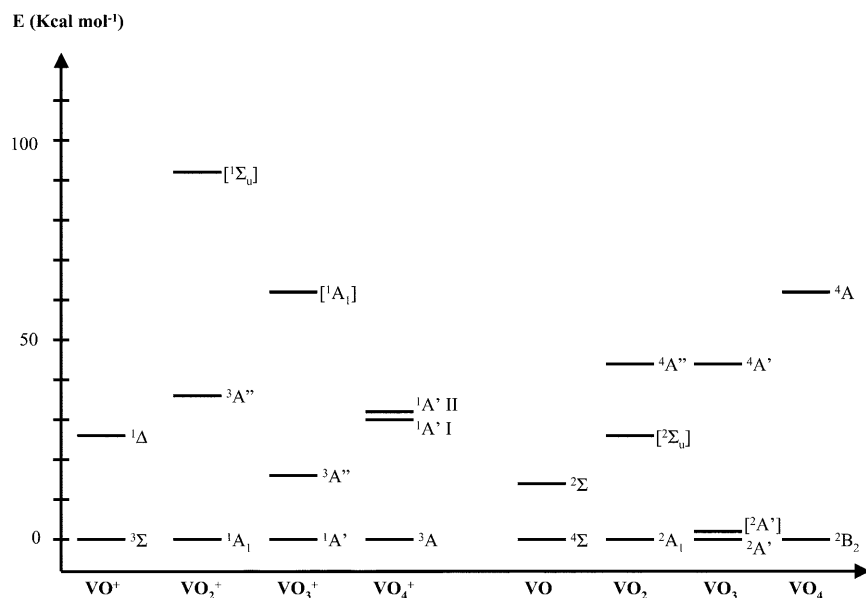


Fig. 4. Relative energy of the different species studied (kcal mol<sup>-1</sup>). The transition states are shown in brackets

$\text{VO}_3$  ( $2A'$ ) presents a typical molecule bifurcation diagram. It is interesting to notice that two different oxygen atoms are found: oxygen 2, whose valence monosynaptic basin appears at  $\eta(\mathbf{r})=0.25$ , and oxy-

gens 1 and 3, splitting at  $\eta(\mathbf{r})=0.35$ . There is a TS ( $2A'$ ) with  $C_{3v}$  symmetry connecting identical minima in the ground state with distances of 1.655 Å and an interconversion barrier height of 62.41 kcal mol<sup>-1</sup>. Their

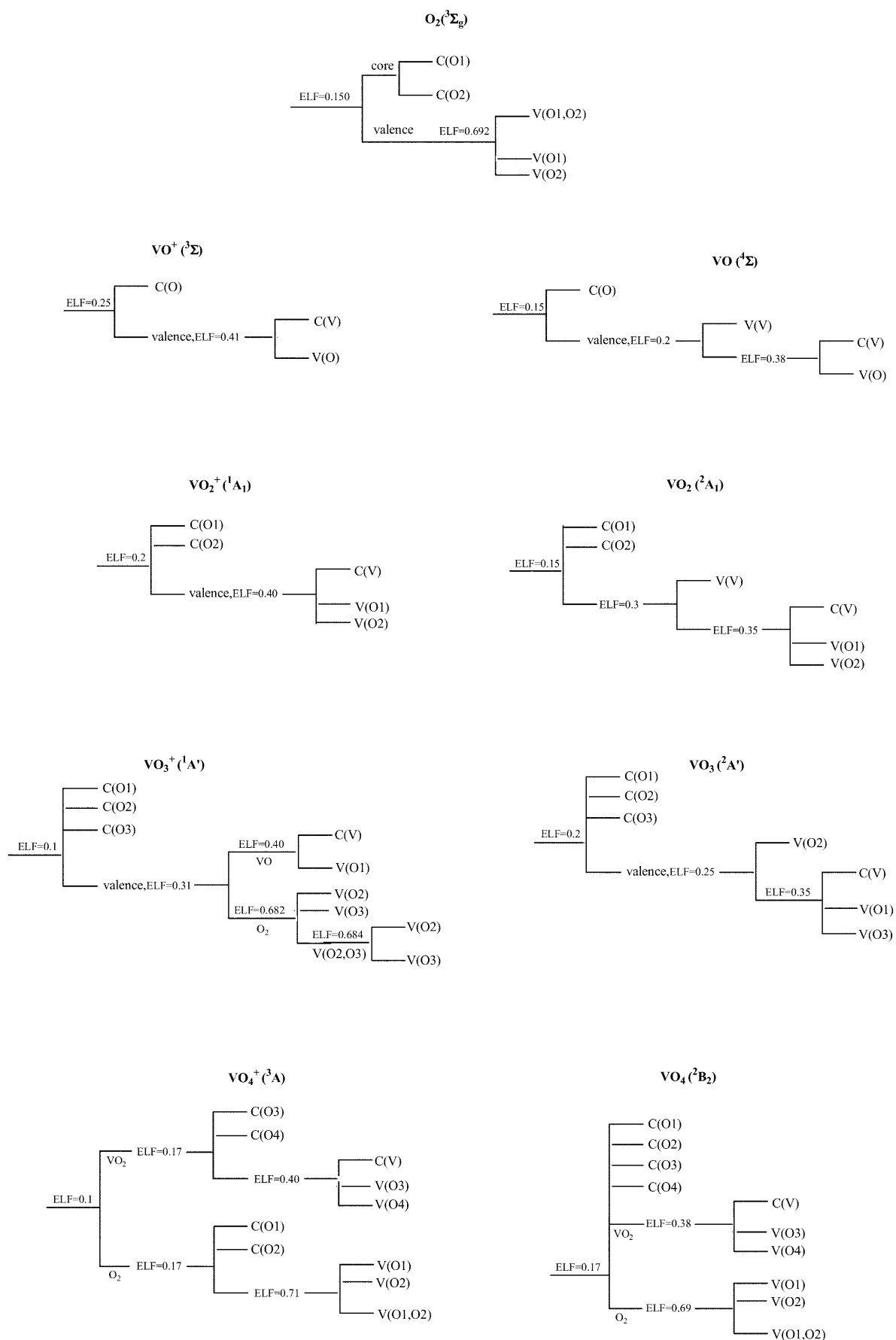


Fig. 5. Localization domain reduction tree diagrams for the most stable vanadium oxide clusters and the oxygen molecule

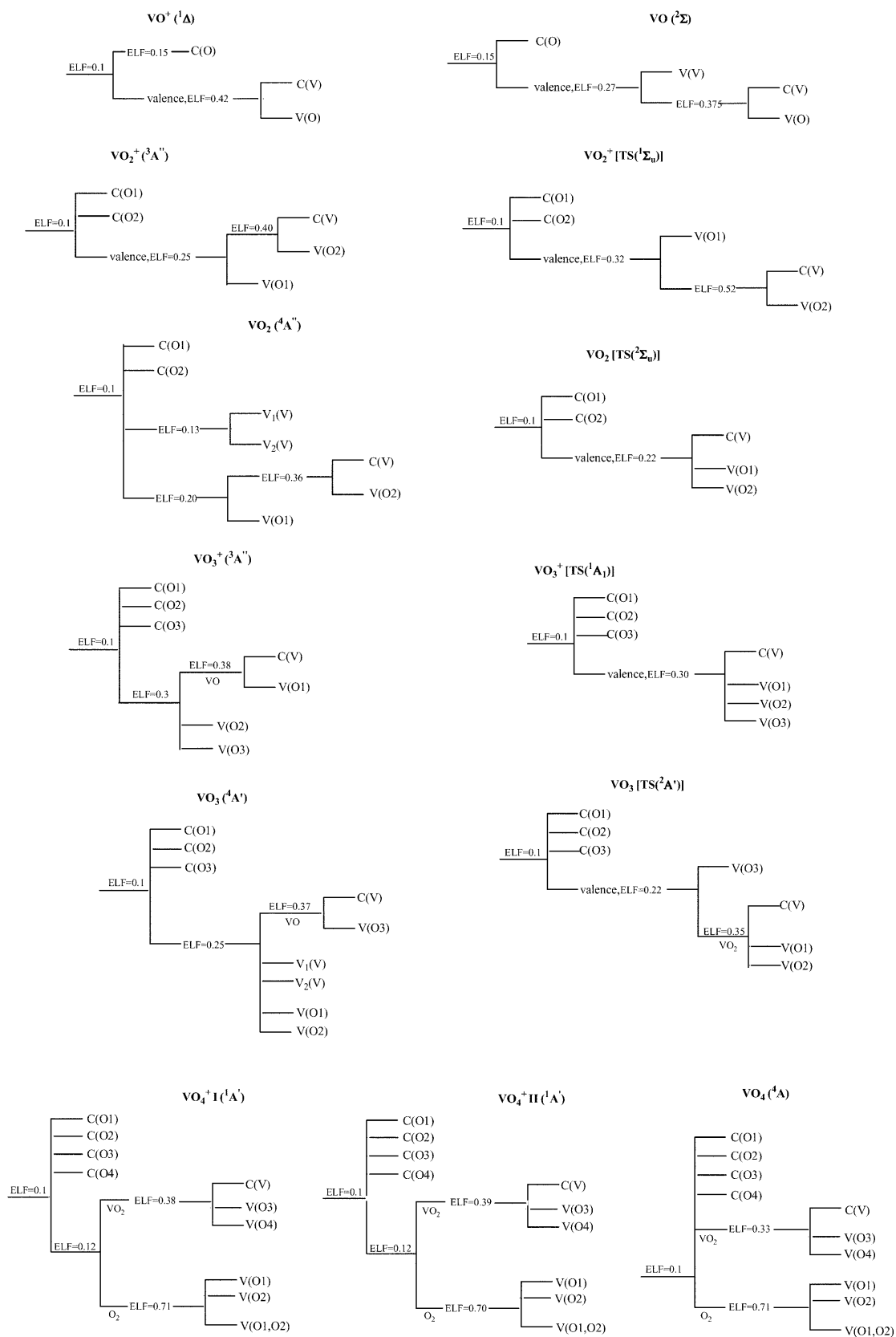


Fig. 6. Localization domain reduction tree diagrams for the excited vanadium oxide clusters



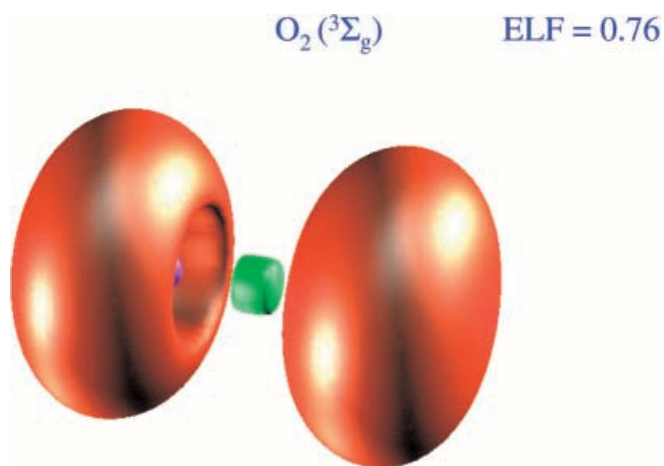


Fig. 7. Electron localization function (ELF) isosurfaces [ $\eta(\mathbf{r}) = 0.76$ ] of  $O_2(^3\Sigma_g)$

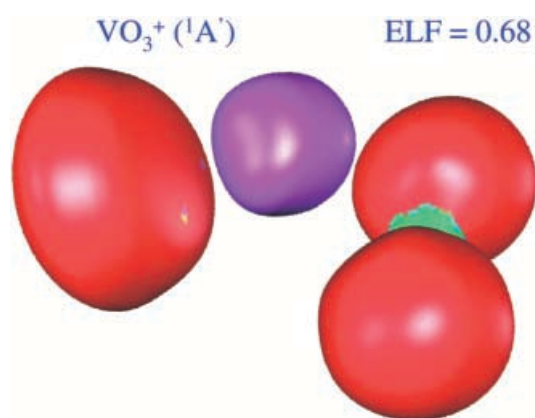


Fig. 8. ELF isosurfaces [ $\eta(\mathbf{r}) = 0.68$ ] of  $VO_3(^1A')$

corresponding tree diagram is similar to fundamental state.

$VO_3(^4A')$  presents a split at  $\eta(\mathbf{r}) = 0.25$  of the valence monosynaptic basins of vanadium and two oxygen atoms and at  $\eta(\mathbf{r}) = 0.37$  the core/valence bifurcation of the vanadium and oxygen atom appears.

#### 4.5 $VO_4^+$ and $VO_4$

The  $VO_4^+(^3A)$  bifurcation tree diagram is typical for interacting fragments, provided that the domain bifurcation occurs before the core/valence bifurcation.  $VO_2$  and  $O_2$  fragments split into their corresponding basins at an ELF value of 0.17. The  $VO_2$  unit coincides with the  $VO_2^+(^1A_1)$  bifurcation diagram, while the  $O_2$  unit bifurcates like the pure molecule, according to the ELF value of 0.71 and the presence of a disynaptic  $V(O1,O2)$  basin. Thus, we can consider the  $VO_4^+$  cluster as an ionic assembly of  $VO_2^+(^1A_1)$  and an  $O_2$  molecule. This description is also evident from the analysis of Fig. 9. The two quasidegenerate excited states I and II  $VO_4^+(^1A')$  present a similar diagram to that of the ground state.

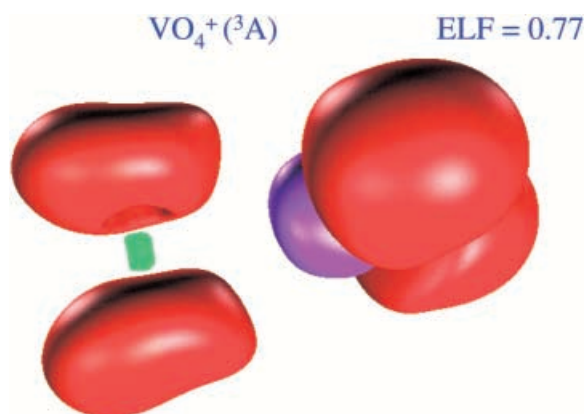


Fig. 9. ELF isosurfaces [ $\eta(\mathbf{r}) = 0.77$ ] of  $VO_4^+(^3A)$

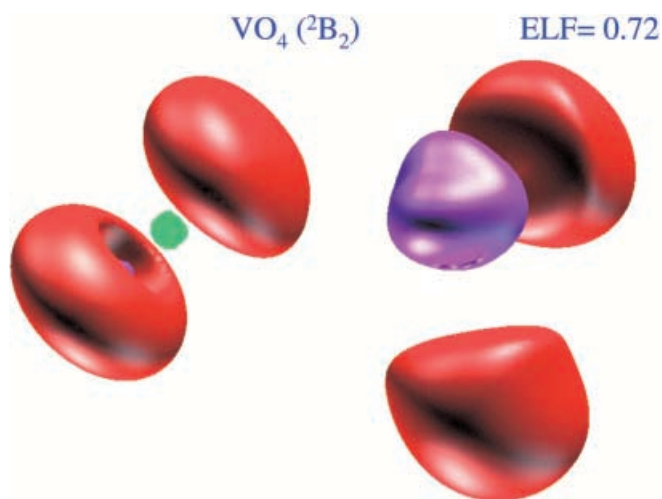


Fig. 10. ELF isosurfaces [ $\eta(\mathbf{r}) = 0.72$ ] of  $VO_4(^2B_2)$

The  $VO_4(^2B_2)$  cluster shows similar behavior to the cation counterpart, with oxygen core basins appearing at the same ELF value of the domain splitting into  $VO_2$  and  $O_2$  units. The  $VO_2$  unit bifurcates in the same way as for  $VO_2(^2A_1)$  without the presence of  $V(V)$ , while the  $O_2$  units behave like the  $O_2$  molecule. We can consider, therefore, an ionic interaction between the two fragments for this cluster. The corresponding isosurface is displayed in Fig. 10. The excited  $VO_4(^4A)$  presents a more evident disynaptic  $V(O1,O2)$  basin.

## 5 Conclusions

In this work an exhaustive study on the bonding properties of  $VO_x^+/VO_x$  ( $x = 1-4$ ) clusters in fundamental and some excited electronic states was carried out. The study was based on the topological analysis of the ELF. Tree diagrams of the corresponding localization domains were obtained. The results of the present work can be summarized as follows.

1. For the fundamental electronic states of  $VO^+/VO$  and  $VO_2^+/VO_2$  clusters, the structural and topological

analysis shows the absence of disynaptic attractor basins between vanadium and oxygen atoms, and the interaction can be described as purely ionic.

2. For  $\text{VO}_3^+$  and  $\text{VO}_4^+/\text{VO}_4$  clusters in the ground and excited electronic states a disynaptic basin is found between O–O; therefore, we conclude that they are in fact small clusters with  $\text{O}_2$  attached.
3. Three different V–O distances are found in these clusters, corresponding to weak and strong ionic interactions.
4. This new theoretical approach opens new ways for a better understanding of the structure, energetics and bonding properties of these vanadium oxide clusters.

*Acknowledgements.* This work was supported by Fundació Caixa Castelló-Bancaixa (project PIA99-02). M.C. would like to thank the Conselleria de Cultura, Educació i Ciència (Generalitat Valenciana) for providing a doctoral grant. B.S. would like to thank the Conselleria de Cultura, Educació i Ciència (Generalitat Valenciana) for providing a grant. Computer facilities of the Servei d'Informàtica (Universitat Jaume I) are acknowledged.

## References

1. Becke AD, Edgecombe KE (1990) *J Chem Phys* 92: 5397
2. Savin A, Nesper R, Wengert S, Fässler TF (1997) *Angew Chem Int Ed Engl* 36: 1809
3. Lewis GN (1916) *J Am Chem Soc* 38: 762
4. Lewis GN (1966) *Valence and the structure of atoms and molecules*. Dover, New York
5. Gillespie RJ, Nyholm RS (1957) *Q Rev Chem Soc* 11: 339
6. Gillespie RJ (1972) *Molecular geometry*. Van Nostrand Reinhold, London
7. Gillespie RJ, Robinson EA (1996) *Angew Chem Int Ed Engl* 35: 495
8. Silvi B, Savin A (1994) *Nature* 371: 683
9. Bader RFW (1990) *Atoms in molecules: a quantum theory*. Oxford University Press, Oxford
10. Savin A, Silvi B, Colonna F (1996) *Can J Chem* 74: 1088
11. Noury S, Colonna F, Savin A, Silvi B (1998) *J Mol Struct* 450: 59
12. Krokidis X, Noury S, Silvi B (1997) *J Phys Chem A* 101: 7277
13. Fuster F, Silvi B (2000) *Chem Phys* 252: 279
14. Mezey PG (1993) *Can J Chem* 72: 928
15. Kohout M, Savin A (1996) *Int J Quantum Chem* 60: 875
16. Fuster F, Silvi B (2000) *Theor Chem Acc* 104: 13
17. Fuster F, Sevin A, Silvi B (2000) *J Phys Chem A* 104: 852
18. Fuster F, Sevin A, Silvi B (2000) *J Comput Chem* 21: 509
19. Frisch MJ, Trucks GW, Schlegel HB, Gill PMW, Johnson BG, Robb MA, Cheeseman JR, Keith T, Peterson GA, Montgomery JA, Raghavachari K, Al-Laham MA, Zakrzewski VG, Ortiz JV, Foresman JB, Cioslowski J, Stefanov BB, Nanayakkara A, Challacombe M, Peng CY, Ayala PY, Chen W, Wong MW, Andres JL, Replogle ES, Gomperts R, Martin RL, Fox DJ, Binkley JS, Defrees DJ, Baker J, Stewart JP, Head-Gordon M, Gonzalez C, Pople JA (1995) *GAUSSIAN94*, revision B1. Gaussian, Pittsburg, Pa
20. Lee C, Yang RG, Parr RG (1988) *Phys Rev B* 37: 785
21. Becke AD (1993) *J Chem Phys* 98: 5648
22. Rassolov VA, Pople JA, Ratner MA, Windus TL (1998) *J Phys Chem* 109: 1223